Preprint
UCRL-JC-150505

Average Nuclear Level Densities and Radiative Strength Functions in $^{56,57}Fe$ from Primary γ-Ray Spectra

E. Tavukcu, J.A. Becker, L.A. Bernstein, P.E. Garrett, M. Guttormsen, G.E. Mitchell, J. Rekstad, A. Schiller, S. Siem, A. Voinov, W. Younes

This article was submitted to 17th International Conference on the Application of Accelerators in Research and Industry CAARI 2002, Denton, TX, November 12-16, 2002

September 26, 2002

U.S. Department of Energy

Lawrence Livermore National Laboratory

Average Nuclear Level Densities and Radiative Strength Functions in ^{56,57}Fe from Primary γ-ray Spectra

E. Tavukcu*†, J.A. Becker†, L.A. Bernstein†, P.E. Garrett†, M. Guttormsen**, G.E. Mitchell*, J. Rekstad**, A. Schiller†**, S. Siem**, A. Voinov‡ and W. Younes†

*North Carolina State University, Raleigh, NC 27695
and Triangle Universities Nuclear Laboratory, Durham, NC 27708
†Lawrence Livermore National Laboratory, Livermore, CA 94551
**Department of Physics, University of Oslo, N-0316 Oslo, Norway
‡Frank Laboratory of Neutron Physics, Joint Institute of Nuclear Research, 141980 Dubna, Russia

Abstract.
An experimental primary γ-ray spectrum vs. excitation-energy bin ($P(E_x, E_\gamma)$ matrix) in a light-ion reaction is obtained for ^{56,57}Fe isotopes using a subtraction method. By factorizing the $P(E_x, E_\gamma)$ matrix according to the Axel-Brink hypothesis the nuclear level density and the radiative strength function (RSF) in ^{56,57}Fe are extracted simultaneously. A step structure is observed in the level density for both isotopes, and is interpreted as the breaking of Cooper pairs. The RSFs for ^{56,57}Fe reveal an anomalous enhancement at low γ-ray energies.

INTRODUCTION

Level densities for many nuclei are known at low excitation energies from counting discrete levels, and at the neutron binding energy B_n from counting neutron resonances. Between those energies, the level density is usually obtained by interpolating experimental data using phenomenological models such as the Fermi-gas model [1, 2]. A method to measure the level density developed by the Oslo Cyclotron group fills the gap between low and high excitations by extracting the level density from zero to close to the neutron binding energy [3]. This extraction method relies on the experimental primary γ-ray spectra, and also provides a simultaneous determination of the radiative strength function (RSF). The RSF is related to average electromagnetic properties of nuclei, and is studied by various methods, such as photonuclear reactions [4] and two-step γ-ray cascades following thermal neutron capture [5]. The extraction method provides determination of both the level density and RSF without assuming the functional form for either, and it can be used as a valuable supplement to other existing techniques.

EXPERIMENTAL DETAILS

The experiment was carried out with 45-MeV ^{3}He particles on a ^{57}Fe target at the Oslo Cyclotron Laboratory. The self-supporting target was enriched to 94.7% and was 3.38-mg/cm^2 thick. Particle-γ coincidences were measured by the CACTUS multidetector array [6] from the (^{3}He,$\alpha\gamma$) and (^{3}He,^{3}He$'\gamma$) reactions. The outgoing charged particles were detected by eight Si(Li) particle telescopes mounted at 45° with respect to the beam axis. Each telescope consists of a front ($\approx$ 150 μm) and an end ($\approx$ 3000 μm) detector. The reaction γ rays were measured by 28 5″×5″ NaI(Tl) detectors, with a total of 15% solid angle coverage.

The measured particle energy was transformed into the initial excitation energy E_x of the residual nucleus from the reaction kinematics. Using the particle-γ coincidences a γ-ray spectrum is constructed for each E_x bin, covering a 238-keV energy range. These spectra were unfolded using the detector response function [7]. A two dimensional primary γ-ray matrix $P(E_x, E_\gamma)$ for the residual nuclei ^{56}Fe and ^{57}Fe from the (^{3}He,α) and (^{3}He,^{3}He$'$) reactions, respectively, was obtained using a subtraction method [8]. The matrix elements below E_x = 4 MeV were eliminated since in this region the reaction mechanism is more likely to be direct than compound. Furthermore, the matrix elements below E_γ = 1.5 MeV were excluded due to (i) electronic issues, and (ii) problems associated with the subtraction method in obtaining the primary γ-ray spectra for low-energy γ rays.

EXTRACTION METHOD

The $P(E_x, E_\gamma)$ matrix represents a γ-ray decay probability distribution once the primary spectrum is normalized to unity at each E_x bin. The $P(E_x, E_\gamma)$ matrix is factorized according to the Axel-Brink hypothesis [9, 10] as a product of the γ-ray transmission coefficient T and the level density ρ at the final energy

$$P(E_x, E_\gamma) \propto T(E_\gamma)\rho(E_x - E_\gamma). \tag{1}$$

The final energy is given by the initial excitation energy minus the emitted γ-ray energy. We derive the functions T at all E_γ and ρ at all excitation energies by a least χ^2 fit to the primary γ-ray data. These derived T's and ρ's together represent one solution that describes the $P(E_x, E_\gamma)$ matrix: there are an infinite number of solutions. Reference [3] shows that all solutions can be obtained from one arbitrary solution by the transformation functions

$$\begin{aligned} \tilde{\rho}(E_x - E_\gamma) &= \rho(E_x - E_\gamma) A \exp(\alpha(E_x - E_\gamma)) \\ \tilde{T}(E_\gamma) &= T(E_\gamma) B \exp(\alpha E_\gamma), \end{aligned} \tag{2}$$

where A, B, and α are free parameters. The T and ρ together are one arbitrary solution, obtained from the χ^2 minimization. The $\tilde{T}$ and $\tilde{\rho}$ are the other solutions obtained by adjusting the free parameters. In order to determine the most probable T and ρ, we optimize the appropriate parameters by using known experimental data, i.e., discrete levels at low E_x and neutron-resonance spacing data at B_n. By fitting the ratio of the known data [11] and our experimental data, i.e., $\tilde{\rho}$ / ρ, with the transformation function $A\exp(\alpha(E_x - E_\gamma))$ in Eq. (2), we determine the parameter A (the magnitude of the level density), and the parameter α (the slope of both the level density and the RSF.) The parameter B, which fixes the magnitude of the RSF, is determined from the average total radiative width $\langle\Gamma\rangle$ of neutron resonances assuming that the main contribution to the radiative strength comes from dipole transitions. The normalization procedure [12] is well defined for ^{57}Fe. Unfortunately, there are no experimental (n,γ) data for ^{56}Fe. Therefore, the level density for ^{56}Fe is normalized using information from the neighboring ^{57}Fe nucleus. A normalization factor is determined by comparing the known level density at B_n [11] with the one obtained from the Fermi-gas model in ^{57}Fe according to the von Egidy parameterization [13]. This factor is multiplied by the von Egidy Fermi-gas level density of ^{56}Fe, which is then employed in the normalization. The magnitude of the RSF for ^{56}Fe (B) is left unnormalized due to lack of experimental data.

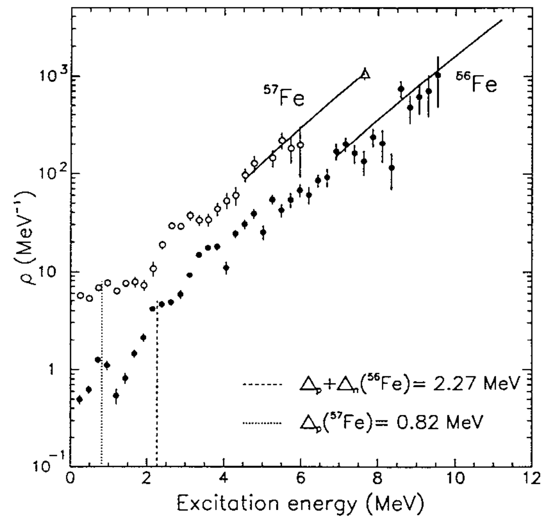

FIGURE 1. Level densities for the ^{56}Fe and ^{57}Fe isotopes. The empty triangle gives the level density at B_n for ^{57}Fe. The Fermi-gas level density is shown by solid lines.

EXPERIMENTAL RESULTS AND DISCUSSIONS

Level Densities

The level densities for ^{56}Fe (solid circles) and ^{57}Fe (empty circles) are shown in Fig. 1. The unfilled triangle at E_x = 7.646 MeV is the level density at B_n obtained from the neutron-resonance spacings data. The normalized Fermi-gas level density, shown by solid lines, describes the shape of the experimental data quite well.

A common feature for both ^{56}Fe and ^{57}Fe in Fig. 1 is the step structure in the level density at low E_x. Discrete-level effects are also pronounced in ^{56}Fe at low excitation. For example, the first bump at 847 keV corresponds to the first excited state, and the second excited state appears at around 2 MeV. Between 2- and 3-MeV excitation, a rather flat behavior is observed, then a step follows this plateau at around 3 MeV. This step structure is a signature for the first pair breaking in ^{56}Fe, and can be associated with the predicted pairing gap parameter Δ. We have calculated the Δ using a three-mass indicator [14], which separates the pairing and single-particle contributions in the odd-even mass staggering. The calculation gives $\Delta_p + \Delta_n$ = 2.27 MeV for ^{56}Fe, and Δ_p = 0.82 MeV for ^{57}Fe, shown in Fig. 1.

The first-pair breaking is expected to take place at $\Delta_p + \Delta_n$ in ^{56}Fe. The calculated $\Delta_p + \Delta_n$ is approximately 0.5 MeV below the energy of the first step at around 3 MeV (see Fig. 1). This is within reasonable agreement with the interpretation of the first pair breaking because, in addition to the pairing energy, an energy on the order of the single-particle energy, is required in order to break one pair and excite one of the nucleons into the lowest unoccupied single-particle state. The step structures associated with further pair breaking become more and more washed out with increasing excitation energy.

The level density in ^{57}Fe is higher than the neighboring even-even nucleus ^{56}Fe. Furthermore, the discrete structure in the level density curve at low E_x in ^{57}Fe is not as pronounced as in the ^{56}Fe case. The reason for these effects is the unpaired neutron in ^{57}Fe. It is generally believed that neighboring odd-odd, odd-even, and even-even isotopes reveal the same level density if a proper shift is applied to the excitation energy [15]. The step structure at around 2 MeV in ^{57}Fe would then correspond to the step observed at around 3 MeV in ^{56}Fe, taking into account an energy shift of about 1 MeV. Accordingly, the steep increase at 2 MeV in ^{57}Fe is interpreted as the first pair breaking.

Radiative Strength Functions

The RSFs for ^{56}Fe and ^{57}Fe are shown in Figs. 2 and 3, respectively. Note that the experimental RSF in ^{56}Fe is given in arbitrary units, i.e., the slope is fixed, but the magnitude remains undetermined. The RSF increases with increasing E_γ above E_γ = 4.5 MeV in ^{56}Fe, as also observed in rare-earth nuclei [12, 16, 17]. The RSF for ^{57}Fe reveals a rather flat structure above E_γ = 3 MeV. In general, the RSF is expected to decrease with decreasing γ-ray energies [12, 16, 17]. In ^{56}Fe, the RSF has a minimum at around E_γ = 4.5 MeV, and increases with decreasing E_γ. A similar enhancement at low energies is observed in ^{57}Fe. We do not believe that this is an artifact of the data reduction since the same behavior was observed in ^{27,28}Si (see below). The RSF might depend, in addition to E_γ, on another parameter of a different origin, such as temperature.

The experimental RSF's are compared to model calculations, assuming that the γ-ray strength is dominated by dipole transitions. For the $E1$ strength, we use two different descriptions: the Lorentzian giant electric dipole resonance (GEDR) model, and the Kadmenskiĭ-Markushev-Furman (KMF) model [18]. The first model is based on Brink's hypothesis, which assumes that giant resonances built on the ground state as well as those built on any excited state have the same size and shape.

In the KMF model [18], the Lorentzian expression is modified in order to reproduce the nonvanishing tail of the GEDR as $E_\gamma \to 0$ by introducing a temperature dependent width of the GEDR.

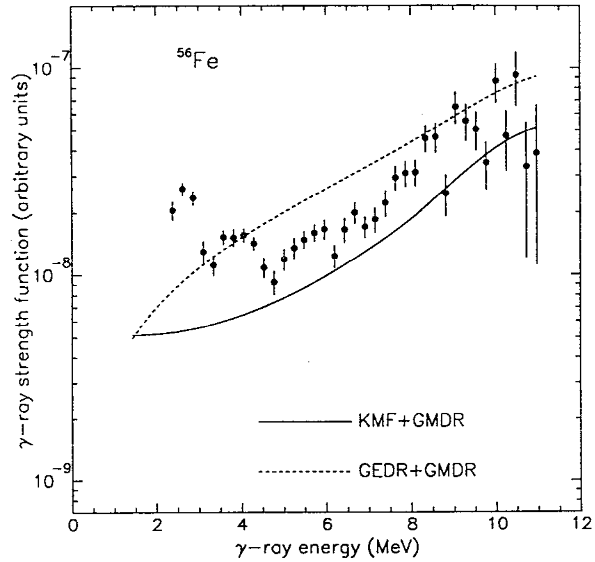

FIGURE 2. Radiative strength function for ^{56}Fe. The experimental RSF (data points) is given in arbitrary units. The models KMF+GMDR and GEDR+GMDR are in absolute units, see text for details.

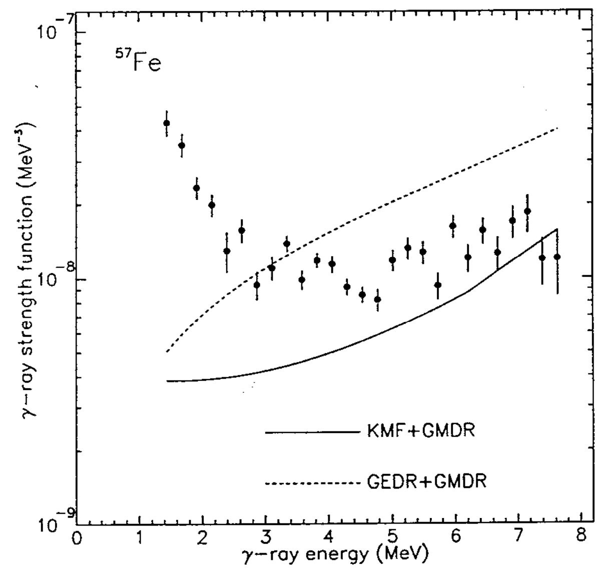

FIGURE 3. Radiative strength function for ^{57}Fe.

For the $M1$ strength, we use a Lorentzian model based on the existence of the $M1$ giant dipole resonance (GMDR), which is assumed to be related to shell-model spin-flip transitions between $l \pm \frac{1}{2}$ single-particle states [19]. Here, the Lorentzian damping width is described as independent of photon energy and temperature.

The GEDR and GMDR parameters are taken from the global parameterization of Ref. [20] for spherical nuclei (A > 50). The calculated $E1$ and $M1$ strengths are summed together in order to compare with the experimental data. These models using different descriptions for the $E1$ strength are denoted by GEDR+GMDR and KMF+GMDR in Figs. 2 and 3. The average contribution of the GMDR strength to the total strength over all the γ-ray energies is $\sim 20\%$. The slope of the RSF for both ^{56}Fe and ^{57}Fe is reproduced with the KMF+GMDR models above E_γ = 4.5 MeV, as well as with the GEDR+GMDR models. Below E_γ = 4.5 MeV, the KMF model tends to follow the data better. Although the KMF model predicts the finite value of the RSF as $E_\gamma \to 0$, it does not reproduce the upward bend at low E_γ [18].

A similar enhancement at the low E_γ is also observed in ^{27,28}Si [21], and ^{96,97}Mo isotopes [22]. For ^{28}Si, levels and level lifetimes, and γ-decay branching ratios are known up to E_x = 9.6 MeV from discrete γ-ray spectroscopy. The γ-ray transmission coefficient for ^{28}Si was calculated from the known lifetime measurements, and compared with the experimental data [21]. Surprising agreement between the experimental and calculated values of the γ-ray transmission coefficient leads us to speculate that the low-energy decay strength in medium-weight and light nuclei is relatively stronger than the corresponding strength in the heavy nuclei.

The presence of this anomaly in the decay strength can be investigated by extracting the multiplicity of the γ rays from different excitation energies. This has not been done yet. If the multiplicity of the γ rays is high, it would provide more confidence that γ rays with low energies are preferred in the decay scheme, and not an artifact of the subtraction method.

SUMMARY

Nuclear level densities and RSFs in ^{56,57}Fe are extracted experimentally from primary γ-ray spectra. These spectra are factorized according to the Axel-Brink hypothesis as a product of the γ-ray transmission coefficient and the level density. The study of several nuclei, such as Si, Fe, Mo and several rare-earth nuclei, has shown that the method works well in different mass regions from light to heavy nuclei. The most interesting finding of the present experiment is the step structure in the level densities of ^{56,57}Fe, which is interpreted as the breaking of the Cooper pairs in the nucleus. With increasing excitation energy, the number of levels increases more smoothly, because there are more broken pairs. An anomalous enhancement in the RSFs in ^{56,57}Fe is observed at low γ-ray energies, which is consistent with results for other light-medium mass nuclei [21, 22]. This effect cannot be explained by the current phenomenological models. The origin of this enhancement remains unknown.

ACKNOWLEDGMENTS

This work was performed under the grant number DE-FG02-97-ER41042 (NCSU). In addition, this work was performed under the auspices of the U.S. Department of Energy by the University of California, Lawrence Livermore National Laboratory under contract No. W-7405-ENG-48. Financial support from the Norwegian Research Council (NFR) is gratefully acknowledged.

REFERENCES

1. Bethe, H. A., *Phys. Rev.*, **50**, 332 (1936).
2. Gilbert, A., and Cameron, A. G. W., *Can. J. Phys.*, **43**, 1446 (1965).
3. Schiller, A., Bergholt, L., Guttormsen, M., , Melby, E., Rekstad, J., and Siem, S., *Nucl. Instrum. Methods Phys. Res. A*, **447**, 498 (2000).
4. Berman, B. L., and Fultz, S. C., *Rev. Mod. Phys.*, **47**, 713 (1975).
5. Bečvář, F., Cejnar, P., Honzátko, J., Konečný, K., Tomandl, I., and Chrien, R. E., *Phys. Rev. C*, **52**, 1278 (1995).
6. Guttormsen, M., Atac, A., Løvhøiden, G., Messelt, S., Ramsøy, T., Rekstad, J., Thorsteinsen, T. F., Tveter, T. S., and Zelazny, Z., *Phys. Scr.*, **T32**, 54 (1990).
7. Guttormsen, M., Tveter, T. S., Bergholt, L., Ingebretsen, F., and Rekstad, J., *Nucl. Instrum. Methods Phys. Res. A*, **374**, 371 (1996).
8. Guttormsen, M., Ramsøy, T., and Rekstad, J., *Nucl. Instrum. Methods Phys. Res. A*, **255**, 518 (1987).
9. Brink, D. M., Ph.D. thesis, Oxford University (1955).
10. Axel, P., *Phys. Rev.*, **126**, 671 (1962).
11. Firestone, R., and Shirley, V. S., *Table of Isotopes*, vol. 1, Wiley, New York, 1996.
12. Voinov, A., Guttormsen, M., Melby, E., Rekstad, J., Schiller, A., and Siem, S., *Phys. Rev. C*, **63**, 044313 (2001).
13. von Egidy, T., Schmidt, H. H., and Behkami, A. N., *Nucl. Phys. A*, **481**, 189 (1988).
14. Dobaczewski, J., Magierski, P., Nazarewicz, W., Satuła, W., and Szymański, Z., *Phys. Rev. C*, **63**, 24308 (2001).
15. Newton, T. D., *Can. J. Phys.*, **34**, 804 (1956).
16. Melby, E., Guttormsen, M., Rekstad, J., Schiller, A., Siem, S., and Voinov, A., *Phys. Rev. C*, **63**, 044309 (2001).
17. Siem, S., Guttormsen, M., Ingeberg, K., Melby, E., Rekstad, J., Schiller, A., and Voinov, A., *Phys. Rev. C*, **65**, 044318 (2002).
18. Kadmenskiĭ, S. G., Markushev, V. P., and Furman, V. I., *Yad. Fiz.*, **37**, 277 (1983), [*Sov. J. Nucl. Phys.* **37**, 165 (1983)].
19. Bohr, A., and Mottelson, B. R., *Nuclear Structure*, vol. 1, World Scientific, Singapore, 1998.
20. Handbook for calculations of nuclear reaction data, Tech. Rep. IAEA-TECDOC-1024, IAEA, Vienna (1998).
21. Guttormsen, M., Melby, E., Rekstad, J., Schiller, A., Siem, S., Lönnroth, T., and Voinov, A. (2002), nucl-ex/0203013.
22. Schiller, A., *et al.*, (unpublished).